Effect of prepulse on fast electron lateral transport at the target surface irradiated by intense femtosecond laser pulses

X. X. Lin (林晓宣),[1] Y. T. Li (李玉同),[1,*] B. C. Liu (刘必成),[1] F. Liu (刘峰),[1] F. Du (杜飞),[1] S. J. Wang (王首钧),[1] X. Lu (鲁欣),[1] L. M. Chen (陈黎明),[1] L. Zhang (张璐),[1] X. Liu (刘勋),[1] J. Wang (王菁),[1] F. Liu (刘峰),[1] X. L. Liu (刘晓龙),[1] Z. H. Wang (王兆华),[1] J. L. Ma (马景龙),[1] Z. Y. Wei (魏志义),[1] and J. Zhang (张杰)[1,2,†]

[1]*Beijing National Laboratory for Condensed Matter Physics, Institute of Physics, Chinese Academy of Sciences, Beijing 100190, People's Republic of China*

[2]*Shanghai Jiao Tong University, Shanghai 200240, People's Republic of China*

(Received 10 March 2010; revised manuscript received 9 July 2010; published 4 October 2010)

The effects of preplasma on lateral fast electron transport at front target surface, irradiated by ultraintense ($>10^{18}$ W/cm^2) laser pulses, are investigated by $K\alpha$ imaging technique. A large annular $K\alpha$ halo with a diameter of ~560 μm surrounding a central spot is observed. A specially designed steplike target is used to identify the possible mechanisms. It is believed that the halos are mainly generated by the lateral diffusion of fast electrons due to the electrostatic and magnetic fields in the preplasma. This is illustrated by simulated electron trajectories using a numerical model.

DOI: 10.1103/PhysRevE.82.046401 PACS number(s): 52.38.Fz, 52.38.Ph

I. INTRODUCTION

The generation and transport of fast electrons are fundamental processes in the fast ignition approach to inertial confinement fusion [1]. Recently the lateral electron transport along the target surface at relativistic intensities has attracted great attention [2–6] due to the important role in the cone guided scheme for fast ignition [7]. For imaging application of laser-driven hard x-ray sources [8,9], the lateral electron transport has also to be controlled because large source size reduces spatial resolution.

The lateral energy transport surrounding a focal spot is a significant and interesting phenomenon, which has attracted much attention for a long time. For example, in the 1980s, the investigations with long pulses (several hundreds of picoseconds) at intensity up to ~10^{16} W/cm^2, indicate that a significant fraction (~30%) of the absorbed laser energy is laterally transported large distance from the laser focal spot [10–13]. Recently, the experimental and theoretical works concentrating on this phenomenon, with short pulses (subpicosecond) at relativistic laser intensity, are reported and several different explanations are proposed [14–17]. The ion emission surrounding the central spot measured by Mckenna *et al.* indicates a significant lateral expansion of electron cloud in thin target foils [14]. Langhoff *et al.* attribute the reduced reflectivity of a probe beam at the circular area around the focal spot to lateral diffusion of returning runaway electrons oscillating across the target surface [15]. Furthermore, Reich *et al.* observe a large weak $K\alpha$ halo with an outer diameter of ~400 μm surrounding a central peak [16], and they believe that the self-generated fields near the target surface result in the lateral electron transport. However, the mechanism detail is still not understood well and the effect of the preplasma is not clear.

In this paper, the lateral electron transport at the front target surface irradiated by intense laser pulses, when a preplasma is formed, is studied by $K\alpha$ imaging technique. The results show that the spatial structure of the $K\alpha$ emission is strongly dependent on the preplasma. Particularly, an annular halo surrounding a central spot is observed for a proper preplasma condition. Furthermore, we use a specially designed target to investigate the origin of the measured $K\alpha$ halo. It is believed that strong self-generated electrostatic and magnetic fields (E and B fields) in the preplasma are responsible for the lateral electron transport.

II. EXPERIMENTAL SETUP

The experiments were carried out using the Xtreme Light II (XL-II) Ti: sapphire laser system at the Institute of Physics, Chinese Academy of Sciences, which can deliver a linearly polarized pulse with energy up to 0.6 J in 60 fs at 800 nm [18]. The laser pulse was focused onto a Cu foil target at an incidence angle of 45° with an $f/3.5$ off-axis parabolic mirror. The diameter of the focal spot was ~4.5 μm at the full width at half maximum (FWHM), in which contained ~35% of the laser energy. The laser intensity was up to 5×10^{18} W/cm^2. The amplified spontaneous emission (ASE) was measured to be ~10^{-5} at ~10 ps before the peak of the main pulse. A prepulse, split from the main pulse, with similar focal spot to that of the main pulse, was used to generate a preplasma.

The main diagnostic was $K\alpha$ imaging technique. A spherically bent quartz 2131 crystal was used to image the Cu $K\alpha$ emission at 8.048 keV onto a 16 bit charge-coupled device (CCD) with a magnification of ~8. The radius of curvature of the crystal was 380 mm. A 30 mm diameter aperture was put in front of the crystal, giving an astigmatism-limited spatial resolution ~19 μm [19]. The energy bandwidth was about 11 eV [20]. The crystal viewed the $K\alpha$ emission at an angle of 48° with respect to the front target normal. The $K\alpha$ yield was measured with a single photon counting PI-LCX CCD, which was set in front of the target at 60° with respect to the target normal. A calibrated magnetic spectrometer with

*ytli@aphy.iphy.ac.cn
†jzhang@aphy.iphy.ac.cn

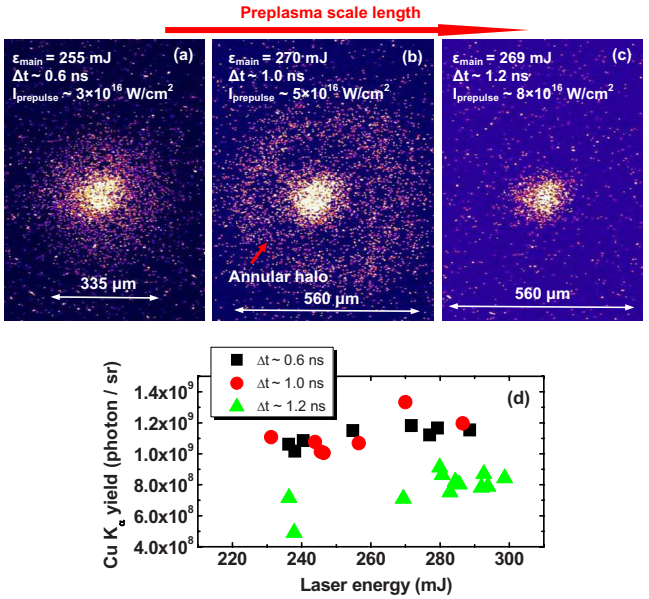

FIG. 1. (Color online) (a)–(c) Typical $K\alpha$ images for three prepulse conditions. ε_{main} is the main laser energy, Δt is the delay time between the prepulse and the main pulse, and $I_{prepulse}$ is the intensity of prepulse. (d) $K\alpha$ yield per steradian measured by the PI-LCX CCD.

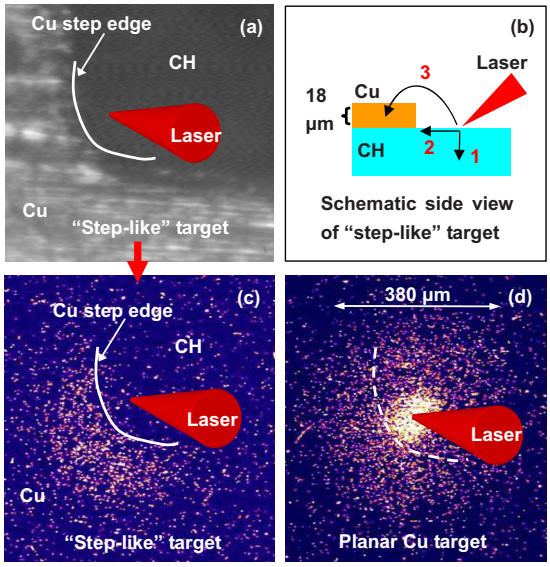

FIG. 2. (Color online) (a) Optical image (top view) and (b) schematic drawing (side view) of the steplike target. The arrows in (b) show the three groups of electrons schematically. $K\alpha$ images of (c) the steplike and (d) planar Cu target obtained with similar laser conditions. The main laser energy is 270 mJ, Δt is 0.6 ns and $I_{prepulse}$ is 3×10^{16} W/cm^2, respectively.

1000 G permanent magnets was used to measure the outgoing electron energy spectrum.

III. RESULTS AND DISCUSSIONS

Figures 1(a)–1(c) show the $K\alpha$ images obtained for three prepulse conditions, when a *p*-polarized laser pulse was focused onto a 50 μm thick Cu foil target. The energy of the main pulse ε_{main} are similar. The preplasma scale length increases from the left to right.

Several features can be seen from the images. A large $K\alpha$ halo surrounding a central bright spot is observed. The $K\alpha$ yield contained in the halo is ~40% relative to the total value. The half-width of the central spot is about 80 μm, which is basically constant for the three conditions and much larger than the laser focal spot. Actually, similar results that the central $K\alpha$ spot is much larger than the laser focal spot have been observed by Stephens *et al.* [21] and Reich *et al.* [16]. They believe that this phenomenon is mainly caused by the spreading of low energy electrons, which laterally drift up to ~50 μm far from the focal spot in the self-generated fields. Collisionless transfer of energy near the critical density to a thermal distribution of background electrons and refluxing of low energy electrons near the front surface also make contributions to the central $K\alpha$ spot [21].

The most striking phenomenon is that the halo structure is strongly dependent on the preplasma conditions. The size of the halo increases with the preplasma scale length. The outer diameter of the halo at 1.0 ns is about 1.5 times larger than that at 0.6 ns. When the preplasma scale length is relatively large at 1.2 ns, the halo almost disappears. Note that halo becomes *annular* with an outer diameter of ~560 μm at 1.0 ns, as shown in Fig. 1(b). Figure 1(d) shows the measured $K\alpha$ yield at the three delays. The yield for 0.6 and 1.0 ns are similar. However, for 1.2 ns it is reduced by ~30–40% relative to the values of 0.6 or 1.0 ns. Since the $K\alpha$ emission from the central bright spot is weak dependent on the preplasma conditions, the reduction is mainly due to the disappearance of the halo at 1.2 ns.

The time-integrated halos must not be excited by the prepulses or the low intensity wings of the main pulses because they strongly depend on the delay Δt and almost vanish when the intensity of the prepulse is relatively high.

Three groups of fast electrons may contribute to the measured halos. The first group penetrates into the solid target with an initial angular spread, and excites $K\alpha$ photons inside the target. The second group is transported laterally as a current along the *initial* target surface due to the confinement of the surface *E* and *B* fields [3,4]. However, this surface current is pronounced only when the incidence angle is large (~70°) and the plasma density profile is steep [4]. The third group is the fast electrons which laterally diffuse in the preplasma *above* the initial target surface. A specially designed steplike target is used to distinguish the contribution of the three groups of electrons. An optical top view and a schematic side view of the target are shown in Figs. 2(a) and 2(b), respectively. An 18 μm thick Cu layer is partially coated on a CH plane substrate. The laser pulse is focused onto the CH surface at a distance of ~60 μm from the Cu step edge. The $K\alpha$ photons are effectively excited only by the fast electrons that laterally diffuse in the preplasma into the Cu layer *above* the CH surface. Figures 2(c) and 2(d) show the comparison of the steplike target with the normal Cu planar target. Both halos have similar structures at the Cu coating region. This indicates that the halo is mainly excited by the third group of fast electrons.

We believe that the observed halo is mainly excited by the fast electrons which laterally drift in the self-generated *B* and

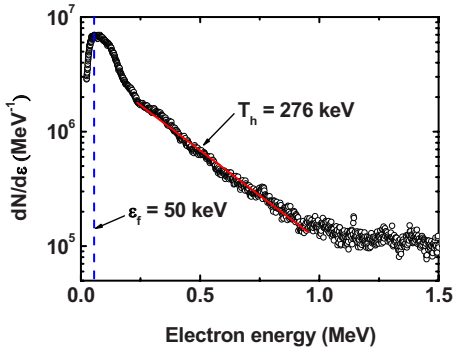

FIG. 3. (Color online) Electron energy spectrum detected at 10° with respect to the front target surface, for the same condition as Fig. 1(b).

E fields in the preplasma and deposit energy far away from the focal spot. In our experiment, a preplasma is generated when the prepulse arrives at the target surface and then expands outward. The following ASE continually heats the expanding preplasma. Before the peak of the fs main pulse, a toroidal, thermoelectric B field can be generated in the preplasma due to the noncollinear electron temperature and density gradients $\nabla T_e \times \nabla n_e$ [22–29]. Moreover, the B field energy is concentrated on the boundary of the preplasma, and expands with the hemispherical plasma bubble [26,28,29]. Previous experimental and theoretical works under various laser conditions suggest that the self-generated B field strength is ~0.4–1 MG [22–29].

In addition, the magnitude of the averaged E field in preplasma [13,28,30], can be estimated from the measured electron spectrum combined with the 2D $K\alpha$ image. Figure 3 shows a typical energy spectrum of the electrons emitted into vacuum for the same condition in Fig. 1(b). The electrons with energy less than 50 keV are quite few because such low energy electrons cannot escape from the preplasma due to the inhibition of the E field. As shown in Fig. 1(b), the annular gap between the central $K\alpha$ spot and the annular halo is corresponding to the region with strong B field, where the plasma bubble boundary locates. Therefore, we take the radius of this gap as the characteristic length of the plasma bubble. This gives an estimation of the average E field $\sim 4\times 10^8$ V/m.

To illustrate the physical picture of this lateral fast electron transport, we perform a 2D cylindrical relativistic simulation of the fast electron trajectories in specified E and B fields. In this model, based on the previous results [23,26,28,29], the distribution of the toroidal B field $B_\theta(r,z)$ is parametrized by

$$B_\theta(r,z) = -B_{\max}[(z^2+r^2)/R_0^2](r/\sqrt{r^2+z^2}), \quad \text{for} \quad \sqrt{(z^2+r^2)} < R_0, \tag{1a}$$

$$B_\theta(r,z) = -B_{\max}[R_0^2/(z^2+r^2)](r/\sqrt{r^2+z^2}), \quad \text{for} \quad R_0 < \sqrt{(z^2+r^2)} < R_1, \tag{1b}$$

$$B_\theta(r,z) = 0, \quad \text{for} \quad \sqrt{(z^2+r^2)} > R_1, \tag{1c}$$

where z and r are the coordinates of the 2D space, $B_{\max}$ is the maximum strength of the B field, R_0 is the radius of the shell where the B field is maximum, and R_1 is outer radius of the B field region. According to Eq. (1), the B field is in the minus theta direction. Moreover, the B field is concentrated around a spherical shell with a radius of R_0, while it becomes weak near the $r=0$ axis where ∇T_e is parallel to ∇n_e. Figure 4(a) shows the constructed B field distribution for the case of Fig. 1(b). The initial target surface is the $z=0$ plane. R_0 and R_1 are set to be 120 and 200 μm, respectively. $B_{\max}$ is set to be 0.5 MG. For simplification, the E field is set to be a fixed strength of $E_z \sim 4\times 10^8$ V/m in the z direction [13,28,30]. The fast electrons, with different initial kinetic energy, ε_f, are launched near assumed critical surface ($r\sim 0$ and $z \sim 25$ μm) with an angle of 15° with respect to the target normal into the fields.

Figure 4(b) shows the fast electron trajectories with various ε_f. It is shown that some fast electrons are laterally deflected in the B field. After a complex lateral drift in the E and B fields, they penetrate again into the solid target surface in an annular region. This can explain the observed annular $K\alpha$ halo. The gap between the central spot and the annular halo can be regarded as the region with strong B field. When the preplasma scale length is increased, the region of the B field expands with the preplasma [26,28,29]. Therefore, the fast electrons can drift further from the central spot. When the scale length is too large, both ∇n_e and ∇T_e become not large enough at far distance away from the central spot, and the self-generated fields become weak. Thus most energetic fast electrons cannot be drawn back to the target surface and excite $K\alpha$ photons. This results in the reduction of the $K\alpha$ yield and the vanishment of the halo for large preplasmas. Moreover, the lower energy electrons are laterally transported and drawn back into the target surface close to the center. This may be one of the possibilities for the phenom-

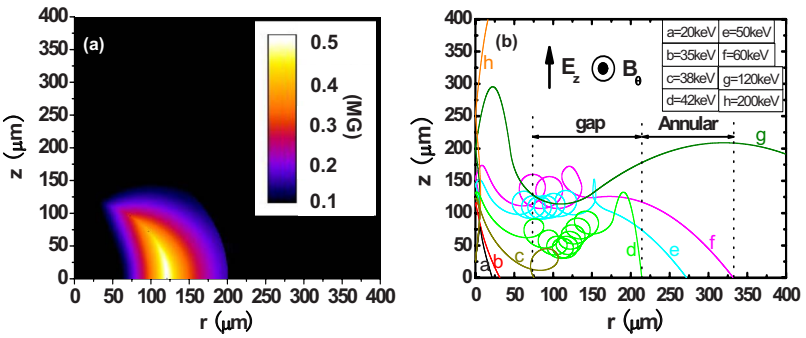

FIG. 4. (Color online) (a) B field distribution according to Eq. (1), when $B_{\max}$ is 0.5 MG, R_0 is 120 μm, and R_1 is 200 μm. (b) Fast electron trajectories. The initial kinetic energy of the fast electrons is changed from 20 to 200 keV for trajectories a to h.

enon that the central $K\alpha$ spot is much larger than the laser focal spot.

IV. SUMMARY

In summary, we have shown that the preplasma conditions significantly affect the lateral fast electron transport and energy deposition at the front target surface. A specially designed steplike target is used to identify the origin of the lateral electron transport. It is suggested that, high contrast laser pulse should be used to optimize the spatial size of the $K\alpha$ source. It also shows a new possible method to estimate the transient B field with an annular halo observed.

ACKNOWLEDGMENTS

This work is supported by the National Nature Science Foundation of China (Grants No. 10925421, No. 10735050, and No. 10734130), National Basic Research Program of China (973 Program) (Grant No. 2007CB815101) and the National High-Tech ICF program.

[1] M. Tabak, J. Hammer, M. E. Glinsky, W. L. Kruer, S. C. Wilks, J. Woodworth, E. M. Campbell, and M. D. Perry, Phys. Plasmas **1**, 1626 (1994).
[2] T. Nakamura, S. Kato, H. Nagatomo, and K. Mima, Phys. Rev. Lett. **93**, 265002 (2004).
[3] M. Chen, Z. M. Sheng, J. Zheng, Y. Y. Ma, M. A. Bari, Y. T. Li, and J. Zhang, Opt. Express **14**, 3093 (2006).
[4] Y. T. Li, X. H. Yuan, M. H. Xu, Z. Y. Zheng, Z. M. Sheng, M. Chen, Y. Y. Ma, W. X. Liang, Q. Z. Yu, Y. Zhang, F. Liu, Z. H. Wang, Z. Y. Wei, W. Zhao, Z. Jin, and J. Zhang, Phys. Rev. Lett. **96**, 165003 (2006).
[5] H. Habara, K. Adumi, T. Yabuuchi, T. Nakamura, Z. L. Chen, M. Kashihara, R. Kodama, K. Kondo, G. R. Kumar, L. A. Lei, T. Matsuoka, K. Mima, and K. A. Tanaka, Phys. Rev. Lett. **97**, 095004 (2006).
[6] X. H. Yuan, Y. T. Li, M. H. Xu, Z. Y. Zheng, Q. Z. Yu, W. X. Liang, Y. Zhang, F. Liu, J. Bernhardt, S. J. Wang, Z. H. Wang, W. J. Ling, Z. Y. Wei, W. Zhao, and J. Zhang, Opt. Express **16**, 81 (2008).
[7] R. Kodama, P. A. Norreys, K. Mima, A. E. Dangor, R. G. Evans, H. Fujita, Y. Kitagawa, K. Krushelnick, T. Miyakoshi, N. Miyanaga, T. Norimatsu, S. J. Rose, T. Shozaki, K. Shigemori, A. Sunahara, M. Tampo, K. A. Tanaka, Y. Toyama, T. Yamanaka, and M. Zepf, Nature (London) **412**, 798 (2001).
[8] D. C. Eder, G. Pretzler, E. Fill, K. Eidmann, and A. Saemann, Appl. Phys. B: Lasers Opt. **70**, 211 (2000).
[9] L. M. Chen, M. Kando, J. Ma, H. Kotaki, Y. Fukuda, Y. Hayashi, I. Daito, T. Homma, K. Ogura, M. Mori, A. S. Pirozhkov, J. Koga, H. Daido, S. V. Bulanov, T. Kimura, T. Tajima, and Y. Kato, Appl. Phys. Lett. **90**, 211501 (2007).
[10] P. A. Jaanimagi, N. A. Ebrahim, N. H. Burnett, and C. Joshi, Appl. Phys. Lett. **38**, 734 (1981).
[11] F. Amiranoff, K. Eidmann, R. Sigel, R. Fedosejevs, A. Maaswinkel, Y. L. Teng, J. D. Kilkenny, J. D. Hares, D. K. Bradley, B. J. MacGowan, and T. J. Goldsack, J. Phys. D **15**, 2463 (1982).
[12] D. W. Forslund and J. U. Brackbill, Phys. Rev. Lett. **48**, 1614 (1982).
[13] J. M. Wallace, Phys. Rev. Lett. **55**, 707 (1985).
[14] P. McKenna, D. C. Carroll, R. J. Clarke, R. G. Evans, K. W. D. Ledingham, F. Lindau, O. Lundh, T. McCanny, D. Neely, A. P. L. Robinson, L. Robson, P. T. Simpson, C. G. Wahlström, and M. Zepf, Phys. Rev. Lett. **98**, 145001 (2007).
[15] H. Langhoff, B. T. Bowes, M. C. Downer, B. X. Hou, and J. A. Nees, Phys. Plasmas **16**, 072702 (2009).
[16] C. Reich, I. Uschmann, F. Ewald, S. Dusterer, A. Lubcke, H. Schwoerer, R. Sauerbrey, E. Forster, and P. Gibbon, Phys. Rev. E **68**, 056408 (2003).
[17] J. F. Seely, C. I. Szabo, P. Audebert *et al.*, Phys. Plasmas **17**, 023102 (2010).
[18] J. Zhang, Y. T. Li, Z. M. Sheng, Z. Y. Wei, Q. L. Dong, and X. Lu, Appl. Phys. B: Lasers Opt. **80**, 957 (2005).
[19] J. A. Koch, Y. Aglitskiy, C. Brown, T. Cowan, R. Freeman, S. Hatchett, G. Holland, M. Key, A. MacKinnon, J. Seely, R. Snavely, and R. Stephens, Rev. Sci. Instrum. **74**, 2130 (2003).
[20] K. U. Akli, M. H. Key, H. K. Chung, S. B. Hansen, R. R. Freeman, M. H. Chen, G. Gregori, S. Hatchett, D. Hey, N. Izumi, J. King, J. Kuba, P. Norreys, A. J. Mackinnon, C. D. Murphy, R. Snavely, R. B. Stephens, C. Stoeckel, W. Theobald, and B. Zhang, Phys. Plasmas **14**, 023102 (2007).
[21] R. B. Stephens, R. A. Snavely, Y. Aglitskiy, F. Amiranoff, C. Andersen, D. Batani, S. D. Baton, T. Cowan, R. R. Freeman, T. Hall, S. P. Hatchett, J. M. Hill, M. H. Key, J. A. King, J. A. Koch, M. Koenig, A. J. MacKinnon, K. L. Lancaster, E. Martinolli, P. Norreys, E. Perelli-Cippo, M. Rabec Le Gloahec, C. Rousseaux, J. J. Santos, and F. Scianitti, Phys. Rev. E **69**, 066414 (2004).
[22] J. A. Stamper, K. Papadopoulos, R. N. Sudan, S. O. Dean, E. A. McLean, and J. D. Dawson, Phys. Rev. Lett. **26**, 1012 (1971).
[23] J. A. Stamper and B. H. Ripin, Phys. Rev. Lett. **34**, 138 (1975).
[24] D. G. Colombant and N. K. Winsor, Phys. Rev. Lett. **38**, 697 (1977).
[25] R. J. Mason, Phys. Rev. Lett. **42**, 239 (1979).
[26] J. A. Stamper, E. A. McLean, and B. H. Ripin, Phys. Rev. Lett. **40**, 1177 (1978).
[27] M. D. J. Burgess, B. Luther-Davies, and K. A. Nugent, Phys. Fluids **28**, 2286 (1985).
[28] C. K. Li, F. H. Seguin, J. A. Frenje, J. R. Rygg, R. D. Petrasso, R. P. J. Town, P. A. Amendt, S. P. Hatchett, O. L. Landen, A. J. Mackinnon, P. K. Patel, V. A. Smalyuk, T. C. Sangster, and J. P. Knauer, Phys. Rev. Lett. **97**, 135003 (2006).
[29] C. K. Li, J. A. Frenje, R. D. Petrasso, F. H. Séguin, P. A. Amendt, O. L. Landen, R. P. J. Town, R. Betti, J. P. Knauer, D. D. Meyerhofer, and J. M. Soures, Phys. Rev. E **80**, 016407 (2009).
[30] P. Mora and R. Pellat, Phys. Fluids **22**, 2300 (1979).